

# Theory of reverse scan square-wave voltammetry influenced by the kinetics of reactant adsorption

Short Communication

Milivoj Lovrić, Šebojka Komorsky-Lovrić

Department of Marine and Environmental Research, "Rudjer Bošković"  
Institute, P.O. Box 180, HR-10002 Zagreb, Hrvatska (Croatia)

Received 28 October 2009; Accepted 11 January 2010

**Abstract:** A model of electrode reaction complicated by slow adsorption of the reactant is developed for square-wave voltammetry with inverse scan direction. The relationship between the dimensionless net peak current and the logarithm of dimensionless rate constant of adsorption is a curve with a minimum and a maximum. For this reason the ratio of real net peak current and the square-root of frequency is a non-linear function of the logarithm of frequency and exhibits either a maximum or a minimum. The frequency of extreme serves for the estimation of the rate constant:  $\log(k_{ads}^*/D^{1/2}) = \log(k_{ads}^*/k_{crit}^*) + 0.5 \log f_{crit}$ , where  $(k_{ads}^*/k_{crit}^*)$  is a critical dimensionless rate constant of adsorption. Square-wave voltammetry is sensitive to the kinetics of adsorption if  $k_{ads}^* < 10^2 \text{ cm s}^{-1}$

**Keywords:** Square-wave voltammetry • Kinetics of adsorption • Adsorption of reactant

© Versita Sp. z o.o.

## 1. Introduction

An adsorption post-wave in dc polarography appears if the reactant of reversible electrode reaction is stabilized by the adsorption to the surface of the working electrode [1,2]. In cyclic voltammetry [3], pulse polarography [4] and square-wave voltammetry [5] the consequence of the reactant adsorption is a post-peak. When the electrode surface is totally covered by the monolayer of the adsorbed reactant before the end of the electrolysis, and if the monolayer does not change the reversibility of the electrode reaction, the reversible main wave will appear in front of the post-wave [6-8]. In theoretical treatments the adsorption process was usually considered to be diffusion-controlled and very fast, always satisfying the adsorption equilibrium [2,3,5,7-9]. However, the influence of adsorption / desorption kinetics was observed in electrode reactions of several ions and compounds, such as fumaric acid on gold electrode [10], thioglycol on mercury electrode [11], osmium complexes [12], ethylene glycol [13] and carbon monoxide on

platinum electrode [14], tetrabutylammonium cations [15], uracil [16] and D-ribose on bismuth electrode [17], chloride [18] and cyanide ions on silver electrode [19], sulfide ions on copper amalgam and mercury electrodes [20] and chloride ions on iron electrode [21]. A theory is developed for slow, non-equilibrated adsorption in linear scan voltammetry [22], chronoamperometry [23,24], electrode impedance measurements [25] and pulse polarography [26].

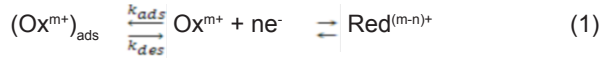
In the present communication, the influence of kinetically controlled adsorption of the reactant in square-wave voltammetry (SWV) with the inverse scan direction is analyzed theoretically. A first order kinetics, which applies to very small reactant concentration and very short electrolysis time [9], is assumed.

\* E-mail: mlovric@irb.hr

## 2. Experimental Procedure

### 2.1. The model

It is assumed that only the reactant of reversible electrode reaction is adsorbed on the surface of stationary, planar electrode:



The reaction scheme (1) can be described by the following system of differential equations, and starting and boundary conditions:

$$\frac{\partial c_{\text{Ox}}}{\partial t} = D \frac{\partial^2 c_{\text{Ox}}}{\partial x^2} \quad (2)$$

$$\frac{\partial c_{\text{Red}}}{\partial t} = D \frac{\partial^2 c_{\text{Red}}}{\partial x^2} \quad (3)$$

$$\frac{d\Gamma_{\text{Ox}}}{dt} = k_{\text{ads}}(c_{\text{Ox}})_{x=0} - k_{\text{des}}\Gamma_{\text{Ox}} \quad (4)$$

$$t = 0, x \geq 0: c_{\text{Ox}} = c_{\text{Ox}}^*, c_{\text{Red}} = 0, \Gamma_{\text{Ox}} = 0 \quad (5)$$

$$t > 0, x \rightarrow \infty: c_{\text{Ox}} \rightarrow c_{\text{Ox}}^*, c_{\text{Red}} \rightarrow 0 \quad (6)$$

$$x = 0: (c_{\text{Ox}})_{x=0} = (c_{\text{Red}})_{x=0} \exp(\varphi) \quad (7)$$

$$\varphi = \frac{nF}{RT} (E - E^0) \quad (8)$$

$$D \left( \frac{\partial c_{\text{Red}}}{\partial x} \right)_{x=0} = \frac{I}{nFS} \quad (9)$$

$$D \left( \frac{\partial c_{\text{Ox}}}{\partial x} \right)_{x=0} = \frac{d\Gamma_{\text{Ox}}}{dt} - \frac{I}{nFS} \quad (10)$$

$$K = \frac{k_{\text{ads}}}{k_{\text{des}}} \quad (11)$$

The meanings of all symbols are given in Table 1. Eq. 4 is a special case of the more general equation  $d\Gamma_{\text{Ox}}/dt = k'_{\text{ads}}(c_{\text{Ox}})_{x=0}(\Gamma_{\text{max}} - \Gamma_{\text{Ox}}) - k_{\text{des}}\Gamma_{\text{Ox}}$ , where  $\Gamma_{\text{max}}$  is the maximum surface concentration of the reactant adsorbed [11,22 - 24]. Eq. 4 applies to very small surface concentration of the adsorbed reactant ( $\Gamma_{\text{Ox}} \ll \Gamma_{\text{max}}$ ). Under this assumption, the interactions between adsorbed species are negligible [22]. This condition can be achieved with very low concentration of the reactant and by the application of reverse scan SWV in which no adsorptive accumulation of the reactant prior to the scan is possible. Note that  $k_{\text{ads}} = k'_{\text{ads}}\Gamma_{\text{max}}$ . The solution of Eqs. 2-4 is obtained by Laplace transforms and the numerical integration [27]. It is the system of recursive formulae:

$$\Phi_1 = (-1 - L_{1,1} + L_{2,1})(A_1 + B_1 - B_2)^{-1} \quad (12)$$

$$\Phi_m = (-1 - L_{1,m} + L_{2,m} - L_{3,m} - L_{4,m} + L_{5,m})(A_m + B_1 - B_2)^{-1} \quad (13)$$

$$m = 2, 3, 4, \dots, 6000 \quad (14)$$

$$\Phi = \frac{I}{nFSc_{\text{Ox}}^* \sqrt{Df}} \quad (15)$$

$$L_{1,1} = \frac{50z_1^2 + k_{\text{des}}^*}{50(z_1 - z_2)z_1} \exp(z_1^2) \text{erfc}(-z_1) \quad (16)$$

$$L_{2,1} = \frac{50z_2^2 + k_{\text{des}}^*}{50(z_1 - z_2)z_2} \exp(z_2^2) \text{erfc}(-z_2) \quad (17)$$

$$A_1 = \frac{(1 + \exp(\varphi_1))\sqrt{2}}{5\sqrt{\pi}} \quad (18)$$

$$B_1 = \frac{(50z_1^2 + k_{\text{des}}^*)M_1}{250(z_1 - z_2)z_1^2\sqrt{2}} \quad (19)$$

$$B_2 = \frac{(50z_2^2 + k_{\text{des}}^*)N_1}{250(z_1 - z_2)z_2^2\sqrt{2}} \quad (20)$$

$$L_{1,m} = \frac{50z_1^2 + k_{\text{des}}^*}{50(z_1 - z_2)z_1} \exp(z_1^2 m) \text{erfc}(-z_1\sqrt{m}) \quad (21)$$

$$L_{2,m} = \frac{50z_2^2 + k_{\text{des}}^*}{50(z_1 - z_2)z_2} \exp(z_2^2 m) \text{erfc}(-z_2\sqrt{m}) \quad (22)$$

$$L_{3,m} = \frac{(1 + \exp(\varphi_m))\sqrt{2}}{5\sqrt{\pi}} \sum_{j=1}^{m-1} \phi_j S_{m-j+1} \quad (23)$$

$$L_{4,m} = \frac{50z_1^2 + k_{\text{des}}^*}{250(z_1 - z_2)z_1^2\sqrt{2}} \sum_{j=1}^{m-1} \phi_j M_{m-j+1} \quad (24)$$

$$L_{5,m} = \frac{50z_2^2 + k_{\text{des}}^*}{250(z_1 - z_2)z_2^2\sqrt{2}} \sum_{j=1}^{m-1} \phi_j N_{m-j+1} \quad (25)$$

$$A_m = \frac{(1 + \exp(\varphi_m))\sqrt{2}}{5\sqrt{\pi}} \quad (26)$$

$$z_1 = -\frac{1}{10\sqrt{2}} [k_{\text{ads}}^* + \sqrt{(k_{\text{ads}}^*)^2 - 4k_{\text{des}}^*}] \quad (27)$$

$$z_2 = -\frac{1}{10\sqrt{2}} [k_{\text{ads}}^* - \sqrt{(k_{\text{ads}}^*)^2 - 4k_{\text{des}}^*}] \quad (28)$$

$$S_1 = 1 \quad (29)$$

$$S_k = \sqrt{k} - \sqrt{k-1} \quad (30)$$

$$M_1 = \exp(z_1^2) \text{erfc}(-z_1) - 1 \quad (31)$$

$$M_k = \exp(z_1^2 k) \text{erfc}(-z_1\sqrt{k}) - \exp(z_1^2(k-1)) \text{erfc}(-z_1\sqrt{k-1}) \quad (32)$$

$$N_1 = \exp(z_2^2) \text{erfc}(-z_2) - 1 \quad (33)$$

$$N_k = \exp(z_2^2 k) \text{erfc}(-z_2\sqrt{k}) - \exp(z_2^2(k-1)) \text{erfc}(-z_2\sqrt{k-1}) \quad (34)$$

$$k_{\text{ads}}^* = \frac{k_{\text{ads}}}{\sqrt{Df}} \quad (35)$$

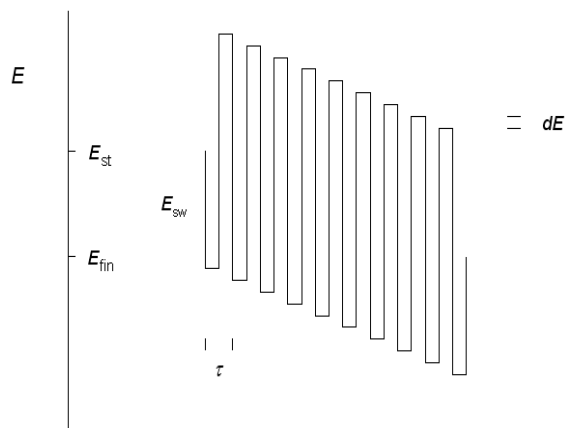
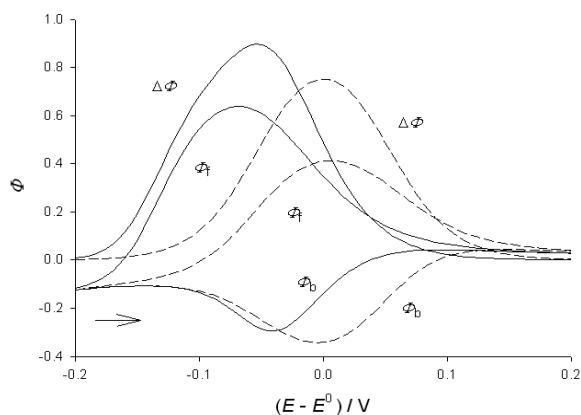
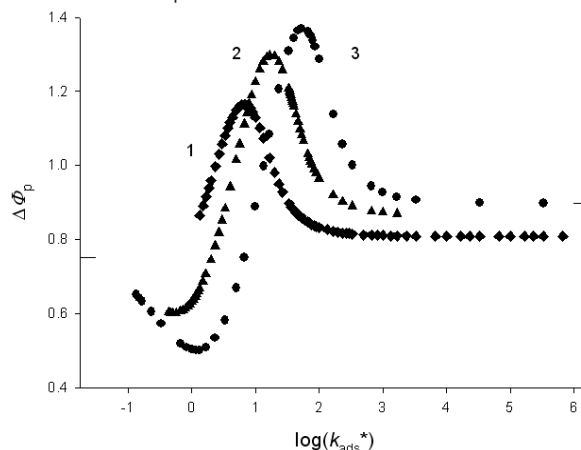
$$k_{\text{des}}^* = \frac{k_{\text{des}}}{f} \quad (36)$$

$$K^* = \frac{K\sqrt{f}}{\sqrt{D}} \quad (37)$$

The solution applies to  $k_{\text{ads}} > 4D/K$ . The time increment is defined as  $\Delta t = (50f)^{-1}$ . This means that each square-wave half-period is divided into 25

**Table 1.** Meanings of symbols

$c_{Ox}$	The reactant concentration
$c_{Ox}^*$	The reactant concentration in the bulk of solution
$(c_{Ox})_{x=0}$	The reactant concentration near the electrode surface
$c_{Red}$	The product concentration
$(c_{Red})_{x=0}$	The product concentration near the electrode surface
D	The common diffusion coefficient
dE	The square-wave potential increment
E	The electrode potential
$E^0$	The standard potential
$E_{sw}$	The square-wave amplitude
$E_{st}$	The square-wave starting potential
$E_p$	The peak potential
F	The Faraday constant
f	The square-wave frequency
$\Phi$	The dimensionless current
$\Phi_p$	The dimensionless peak current
$\Gamma_{Ox}$	The surface concentration of adsorbed reactant
I	The current
$\Delta I_p$	The net peak current
$k_{ads}$	The rate constant of adsorption
$k_{ads}^*$	The dimensionless rate constant of adsorption
$k_{des}$	The rate constant of desorption
$k_{des}^*$	The dimensionless rate constant of desorption
K	The equilibrium constant of adsorption
$K^*$	The dimensionless equilibrium constant of adsorption
n	The number of electrons
R	The gas constant
S	The electrode surface area
t	The time
$\Delta t$	The time increment
x	The distance perpendicular to the electrode surface

**Scheme 1.** Excitation signal of the square-wave voltammetry.  $E_{sw}$  pulse height, dE potential increment,  $\tau$  staircase period,  $E_{st}$  starting potential,  $E_{fin}$  final potential.**Figure 1.** Square-wave voltammograms of electrode reaction (1) unaffected by the reactant adsorption ( $K=0$ ) (a broken line), and influenced by the fast, equilibrated adsorption of reactant ( $K=33.33$  and  $k'_{ads} > 10^3$ ) (a full line).  $E_{st} = -0.3$  V vs  $E^0$ , dE = 5 mV and  $E_{sw} = 50$  mV. A net response ( $\Delta\Phi$ ) and its forward ( $\Phi_f$ ) and backward ( $\Phi_b$ ) components are shown.**Figure 2.** Dependence of dimensionless net peak current of square-wave voltammograms of electrode reaction (1) on the logarithm of dimensionless rate constant of the reactant adsorption.  $K^* = 3.33$  (1,  $\blacklozenge$ ), 10 (2,  $\blacktriangle$ ) and 33.33 (3,  $\bullet$ ). All other parameters are as in Fig. 1.

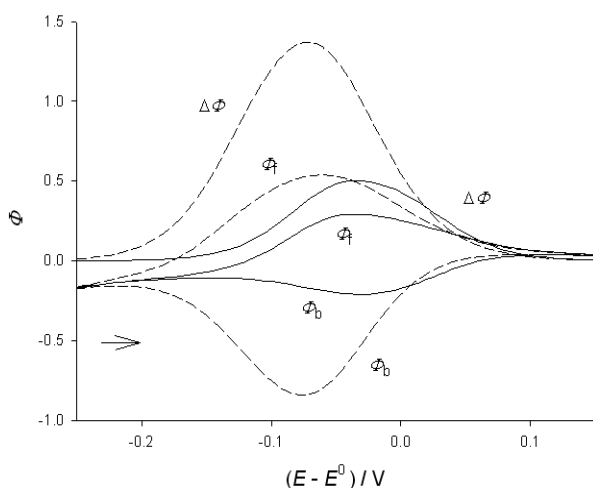


**Figure 3.** Square-wave voltammograms of electrode reaction (1) influenced by kinetically controlled adsorption of reactant.  $K^* = 33.33$  and  $k_{ads}^* = 1$  (a full line) and 53.33 (a broken line). All other parameters are as in Fig. 1.

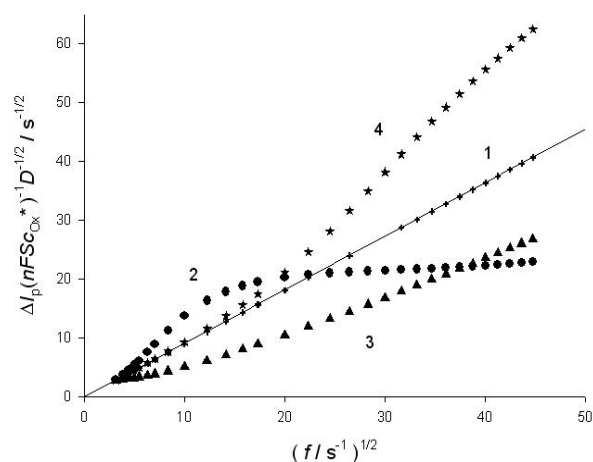


**Figure 4.** Dependence of normalized net peak current on the square-root of frequency.  $K = 0.01$  cm,  $k_{ads} / \text{cm s}^{-1} > 10^4$  (1), = 1.6 (2), 0.03 (3) and 30 (4). All other parameters are as in Fig. 1.

increments [28]. The electrode potential  $E_m$  is changed according to the Scheme 1. For the electrode reaction 1 and the initial conditions (5), the usual starting potential is higher than the standard potential and the scan direction is negative. So, the inverse scan direction is positive, starting from the potential lower than the standard potential. In square-wave voltammetry (SWV) on static mercury drop electrode it is assumed that the electrode appears instantaneously in its full volume at the moment  $t = 0$ . In this moment its surface is free of any adsorbate and the reactant concentration at the electrode surface is equal to the bulk concentration. This is expressed by the condition (5). Furthermore, in the reverse scan SWV the starting potential is much lower than the standard potential and the adsorbed reactant is not stable on the electrode surface.

### 3. Results and Discussion

Square-wave voltammograms of electrode reaction 1, recorded with the positive scan direction starting from  $-0.3$  V vs  $E^0$ , are shown in Fig. 1. If the reactant adsorption is negligible ( $K^* = 0$ ), the net peak potential is equal to the standard potential and the dimensionless net peak current is 0.75175 for the given square-wave amplitude (a broken line). The maximum of the dimensionless forward, oxidative component of the net response is 0.4116 and it appears at 0.005 V vs  $E^0$ . The minimum of the backward, reductive component is  $-0.3435$ , which appears at  $-0.005$  V vs  $E^0$ . Both components are negative at the starting potential because of the reduction of reactant that is initially present in the bulk of solution.

Adsorption of the reactant depends on the dimensionless equilibrium constant  $K^* = K\sqrt{f/D}$  and the dimensionless rate constant  $k_{ads}^* = k_{ads}/\sqrt{Df}$ . If  $K^* = 33.33$  and  $k_{ads}^* > 10^5$ , the adsorption is strong, fast and reversible, so that the equilibrium is continuously maintained at the electrode surface. These dimensionless parameters correspond to  $K = 10^{-2}$  cm,  $D = 9 \times 10^{-6}$  cm<sup>2</sup> s<sup>-1</sup>,  $f = 100$  s<sup>-1</sup> and  $k_{ads} > 3 \times 10^3$  cm s<sup>-1</sup>. Square-wave voltammogram influenced by the strong and equilibrated adsorption is shown in Fig. 1 by the full line. The dimensionless net peak current is increased to 0.8970, and the net peak potential is shifted to  $-0.055$  V vs  $E^0$ . Also, the forward component is enhanced ( $\Phi_{p,f} = 0.6379$ ,  $E_{p,f} = -0.070$  V vs  $E^0$ ), while the backward component is diminished ( $\Phi_{p,b} = -0.2945$ ,  $E_{p,b} = -0.040$  V vs  $E^0$ ) with regards to the response shown by a broken line in Fig. 1. Quantitative differences between the square-wave voltammograms in Fig. 1 are significant, but qualitatively these two responses are similar and no information on the adsorption process can be obtained from the form of square-wave voltammogram, particularly if the standard potential is not known exactly.

Fig. 2 shows relationships between dimensionless square-wave voltammetric net peak currents and the logarithm of dimensionless rate constant of reactant adsorption. In these calculations it was assumed that the square-wave frequency was constant. The range of arguments was restricted by the condition  $k_{ads}^* > 4/K^*$ . The relationships in Fig. 2 are characterized by the minima and maxima. The arguments of these extremes depend on the dimensionless equilibrium constant. If  $K^* = 33.33$ , the minimum appears at  $\log k_{ads}^* = 0.0669$ , and the maximum for  $\log k_{ads}^* = 1.727$ . If  $K^* = 10$ , the abscissas of the minimum and maximum are  $\log k_{ads}^* = -0.301$  and  $\log k_{ads}^* = 1.222$ , respectively, and if  $K^* = 3.33$  the maximum appears at  $\log k_{ads}^* = 0.8239$ .

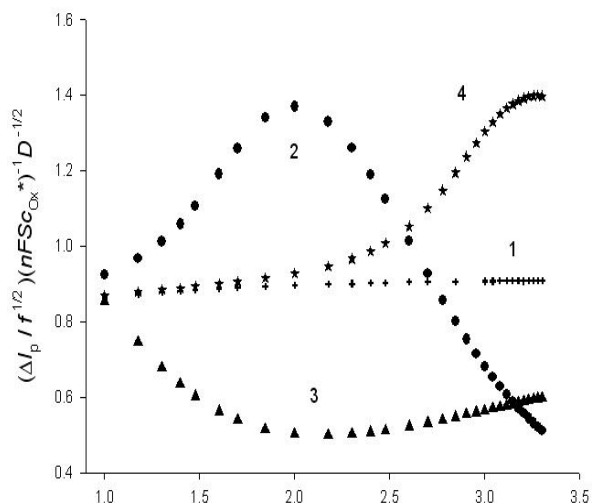


**Figure 5.** Dependence of dimensionless ratio of net peak current and the square-root of frequency on the logarithm of frequency.  $K = 0.01$  cm,  $k_{ads} / \text{cm s}^{-1} > 10^4$  (1), 1.6 (2), 0.03 (3) and 30 (4). All other parameters are as in Fig. 1.

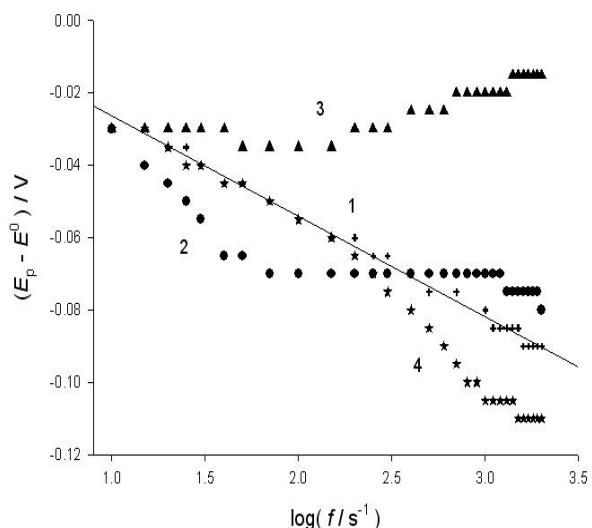


**Figure 6.** Dependence of the net peak potential on the logarithm of frequency.  $K = 0.01$  cm,  $k_{ads} / \text{cm s}^{-1} > 10^4$  (1), 1.6 (2), 0.03 (3) and 30 (4). All other parameters are as in Fig. 1.

Short lines in the left and right sides of Fig. 2 correspond to dimensionless net peak currents of voltammograms shown in Fig. 1. These results indicate that under the influence of adsorption kinetics there is no linear dependence of the net peak currents on the square-root of frequency.

The forms of square-wave voltammograms that correspond to the minimum and maximum of curve 3 in Fig. 2 are shown in Fig. 3. At the minimum, all dimensionless peak currents are smaller than in the absence of adsorption ( $\Delta\Phi_p = 0.5025$ ,  $\Phi_{p,f} = 0.2921$  and  $\Phi_{p,b} = -0.2106$ ) and all peak potentials are lower than the standard potential:  $E_p = -0.035$  V,  $E_{p,f} = -0.035$  V

and  $E_{p,b} = -0.030$  V (a full line). At the maximum, the dimensionless net peak current is higher than in Fig. 1 ( $\Delta\Phi_p = 1.37$ ) because of the enhanced reductive component ( $\Phi_{p,b} = -0.8439$ ) (a broken line). The ratio  $\Phi_{p,f} / \Phi_{p,b}$  changes from  $-2.166$  in Fig. 1 (a full line), to  $-0.637$  in Fig. 3 (a broken line). Also, the peak potentials of the net response and its backward component are lower than the corresponding potentials in Fig. 1:  $E_p = -0.070$  V,  $E_{p,f} = -0.060$  V and  $E_{p,b} = -0.075$  V. If the variation of square-wave frequency causes the change of voltammograms that is similar to the one shown in Figs. 1 and 3, this may be the qualitative indication of the influence of kinetics of adsorption.

If the reactant adsorption is fast and reversible, the dimensionless net peak current ( $\Delta\Phi_p$ ) is independent of the dimensionless rate constant  $k_{ads}^*$  (see Fig. 2 for  $k_{ads}^* > 10^5$ ) and the real net peak current is linear function of the square-root of frequency:

$$\Delta I_p = \Delta\Phi_p nFSc_{ox}^* \sqrt{Df} \quad (38)$$

This is shown by the straight line (1) in Fig. 4. However, if by increasing the frequency  $k_{ads}^*$  is diminished below  $10^3$ ,  $\Delta\Phi_p$  either increases, or decreases with frequency and  $\Delta I_p$  declines from the straight line (38). This can be seen in curves (2) – (4) in Fig. 4. The ratio of real net peak current and the square-root of frequency as a function of logarithm of frequency is shown in Fig. 5. These relationships may exhibit either maximum, or minimum and the abscissas of these extremes can be used for the estimation of the adsorption rate constants. For instance, the curve (2) in Fig. 5 is in maximum for  $\log(f_{max} / \text{s}^{-1}) = 2$ . This critical frequency is connected to the dimensionless rate constant  $(k_{ads}^*)_{max}$  for which the dimensionless net peak current  $\Delta\Phi_p$  is in maximum:

$$\frac{k_{ads}}{\sqrt{Df_{max}}} = (k_{ads}^*)_{max} \quad (39)$$

In Fig. 2 it can be seen that  $\log(k_{ads}^*)_{max} = 1.2 \pm 0.5$ , which applies to  $3.33 \leq K^* \leq 33.33$ . So, the ratio of the adsorption rate constant and the square-root of the diffusion coefficient is defined by the following equation:

$$\log \frac{k_{ads}}{\sqrt{D}} = \frac{1}{2} \log f_{max} + 1.2 \pm 0.5 \quad (40)$$

Eq. 40 applies to  $0.001 \leq K / \text{cm} \leq 0.01$ .

Fig. 6 shows the dependence of net peak potential on the logarithm of frequency. If the adsorption is fast and reversible, this relationship is linear and its slope is  $\partial E_p / \partial \log f = -2.3 RT / 2nF$  [28]. This is shown by the straight line (1). The curves (2) and (4) show that the slope  $\partial E_p / \partial \log f$  is steep in the frequency range in which the ratio  $\Delta I_p / \sqrt{f}$  increases

with frequency, and that the slope is negligible if this ratio decreases with frequency (see Fig. 5). So, the non-linear dependence of the net peak potential on the logarithm of frequency is the indication of possible influence of adsorption kinetics. Note that in SWV the net peak potential changes in discrete values equal to the potential step increment  $\Delta E$ , which is 5 mV in Fig. 6 [28].

## 4. Conclusions

These results show that in square-wave voltammetry of electrode reaction (1) the kinetics of reactant adsorption can be noticed if  $k_{ads}^* < 10^3$ . Assuming that  $D = 10^{-5} \text{ cm}^2 \text{ s}^{-1}$  and  $f = 10^3 \text{ s}^{-1}$ , the

kinetics is measurable if  $k_{ads} < 10^2 \text{ cm s}^{-1}$ . This is rather low sensitivity because the rate constants of majority of adsorption processes are higher than  $10^3 \text{ cm s}^{-1}$  [11,15,16,29,30]. However, the purpose of this work is to report the criteria for distinguishing diffusion controlled and kinetically controlled post-waves in the reverse scan square-wave voltammetry. This can be an useful criteria with wide potential in recognition of very slow adsorption processes. The model is maximally simplified and does not consider competitive adsorption appearing in the mixture of surface active substances, or the influence of electrode material on the adsorption process.

## References

- [1] M. Heyrovsky, S. Vavřička, R. Heyrovská, *Electroanal. Chem. Interfac. Electrochem.* 46, 391 (1973)
- [2] R. Guidelli, F. Pergola, *J. Electroanal. Chem.* 84, 225(1977)
- [3] R.H. Wopschall, I. Shain, *Anal. Chem.* 39, 1514 (1967)
- [4] J.B. Flanagan, K. Takahashi, F.C. Anson, *J. Electroanal. Chem.* 85, 257 (1977)
- [5] M. Lovrić, Š. Komorsky-Lovrić, *J. Electroanal. Chem.* 248, 239 (1988)
- [6] M.O. Bernard, C. Bureau, J.M. Soudan, G. Lecayon, *J. Electroanal. Chem.* 431, 153 (1997)
- [7] K. Kobayashi, *Chem. Letters* 1243 (1988)
- [8] M. Lovrić, *J. Electroanal. Chem.* 170, 143 (1984)
- [9] E. Laviron, L. Roullier, *J. Electroanal. Chem.* 443, 195 (1998)
- [10] H. Noda, K. Ataka, L.J. Wan, M. Osawa, *Surf. Sci.* 427-428, 190 (1999)
- [11] A. Szulborska, A. Baranski, *J. Electroanal. Chem.* 377, 269 (1994)
- [12] J.D. Tirado, D. Acevedo, R.L. Bretz, H.D. Abruña, *Langmuir* 10, 1971 (1994)
- [13] Y.J. Fan, Z.Y. Zhou, C.H. Zhen, C.J. Fan, S.G. Sun, *Electrochim. Acta* 49, 4659 (2004)
- [14] M. Heinen, Y.X. Chen, Z. Jusys, R.J. Behm, *Electrochim. Acta* 53, 1279 (2007)
- [15] K. Laes et al., *J. Electroanal. Chem.* 569, 241 (2004)
- [16] H. Kasuk, G. Nurk, K. Lust, E. Lust, *J. Electroanal. Chem.* 550-551, 13 (2003)
- [17] A. Janes, K. Lust, E. Lust, *J. Electroanal. Chem.* 548, 27 (2003)
- [18] B.M. Jović, V.D. Jović, D.M. Dražić, *J. Electroanal. Chem.* 399, 197 (1995)
- [19] N.A. Rogozhnikov, R.Y. Beck, *J. Electroanal. Chem.* 457, 31 (1998)
- [20] A. Basa, T. Krogulec, A.S. Baranski, *J. Electroanal. Chem.* 463, 200 (1999).
- [21] D.M. Dražić, Lj. Vračar, V.J. Dražić, *Electrochim. Acta* 39, 1165 (1994)
- [22] E. Laviron, *J. Electroanal. Chem.* 140, 247 (1982)
- [23] E. Bosco, *J. Electroanal. Chem.* 346, 433 (1993)
- [24] I. Bhugun, F.C. Anson, *J. Electroanal. Chem.* 439, 1 (1997)
- [25] V.V. Pototskaya, N.E. Evtushenko, O.I. Gichan, *Russian J. Electrochem.* 40, 424 (2004)
- [26] Š. Komorsky-Lovrić, M. Lovrić, *Electrochim. Acta* 30, 1143 (1985)
- [27] R.S. Nicholson, M.L. Olmstead, In J.S. Matson, H.B. Mark, H.C. MacDonald (Eds.), *Electrochemistry: Calculations, Simulations and Instrumentations*, Vol. 2 (Marcel Dekker, New York, 1972) 236.
- [28] V. Mirčeski, Š. Komorsky-Lovrić, M. Lovrić, *Square-wave voltammetry* (Springer, Berlin, 2007)
- [29] W. Lorenz and F. Möckel, *Z. Elektrochem.* 60, 507 (1956)
- [30] R.D. Armstrong, W.P. Race, H.R. Thirsk, *J. Electroanal. Chem.* 16, 517 (1968)